

# HIGH TEMPERATURE THERMAL CONDUCTIVITY MEASUREMENT APPARATUS

Markus Selzer<sup>(1)</sup>, Karl Keller<sup>(2)</sup>, Thomas Reimer<sup>(1)</sup>, Heiko Ritter<sup>(3)</sup>

<sup>(1)</sup> *DLR, Institute of Structures and Design*  
*Pfaffenwaldring 38-40*  
*70569 Stuttgart, Germany*  
[Markus.Selzer@dlr.de](mailto:Markus.Selzer@dlr.de)  
[Thomas.Reimer@dlr.de](mailto:Thomas.Reimer@dlr.de)

<sup>(2)</sup> *Keltec*  
*Jägerweg 2*  
*82139 Starnberg, Germany*  
[Keller@Keltec.eu](mailto:Keller@Keltec.eu)

<sup>(3)</sup> *European Space Agency (ESA) - ESTEC*  
*Noordwijk, The Netherlands*  
[Heiko.Ritter@esa.int](mailto:Heiko.Ritter@esa.int)

## 1 INTRODUCTION

Reliable dimensioning of highly efficient thermal protection for entry or re-entry applications depends on an accurate knowledge of the thermal conductivity of the considered materials. The fibre and foam insulations, as well as ablator char, used in such thermal protection systems are porous materials, where the thermal conductivity varies with both, applied temperature and ambient pressure. Precise thermal conductivity measurements in the lower temperature range and for isotropic insulations are state-of-the art. The transfer of well-established lower temperature measurement principles to very high temperatures and to non-isotropic insulations is a challenge. The German aerospace center (DLR) owns a facility of adequate size which enables thermal conductivity measurements at high temperatures up to 1600°C and for controllable ambient pressures between 1 mbar and ambient pressure. This facility has been used in previous projects, however, the quality of steady state thermal conductivity measurements was not satisfactorily in particular for reduced pressure levels. This is caused by uncontrolled lateral heat exchanges at the test specimen surface. Control of these lateral heat exchanges is therefore the key for improvement of measurement accuracy.

With this in mind, a test setup for measurements under varying temperatures up to 1600°C and for pressures between 1 mbar and ambient pressure has been developed as part of ESA's Innovation Triangle Initiative. This test setup is not only applicable to today's most advanced insulations, i.e. to nanoporous insulations and to anisotropic insulation systems like internal multiscreen insulation (IMI), but also to the direct measurement of ablator char thermal conductivity. At first, the measurement of thermal conductivity and the therefore developed test setup HitCon are described. Next, the results from a measurement campaign, conducted to verify the functionality of the design, are shown, followed by sensitivity analysis for further improvement of the test setup.

## 2 THERMAL CONDUCTIVITY MEASUREMENT

Thermal conductivity  $\lambda$  is defined as

$$\lambda = \frac{Q}{A} / \frac{\Delta T}{\Delta L} \quad (1)$$

where  $Q$  is the amount of heat passing through a cross section area  $A$  causing a temperature difference  $\Delta T$  over a distance  $\Delta L$  (compare to Fig. 2).  $Q/A$  is therefore the heat flux which is causing the thermal gradient  $\Delta T/\Delta L$ . The measurement of thermal conductivity, therefore, always involves the measurement of a heat flux and of a temperature gradient. The main difficulty is always associated with the heat flux measurement. Where the heat flux is measured directly (for example measuring the electrical power going into a heater) the measurement is called absolute. Where the heat flux measurement is done indirectly (by comparison) the method is called comparative. In all cases the entire heat flux must be uniaxial, that is, it has to flow solely through the sample (and the references, in the comparative case). This

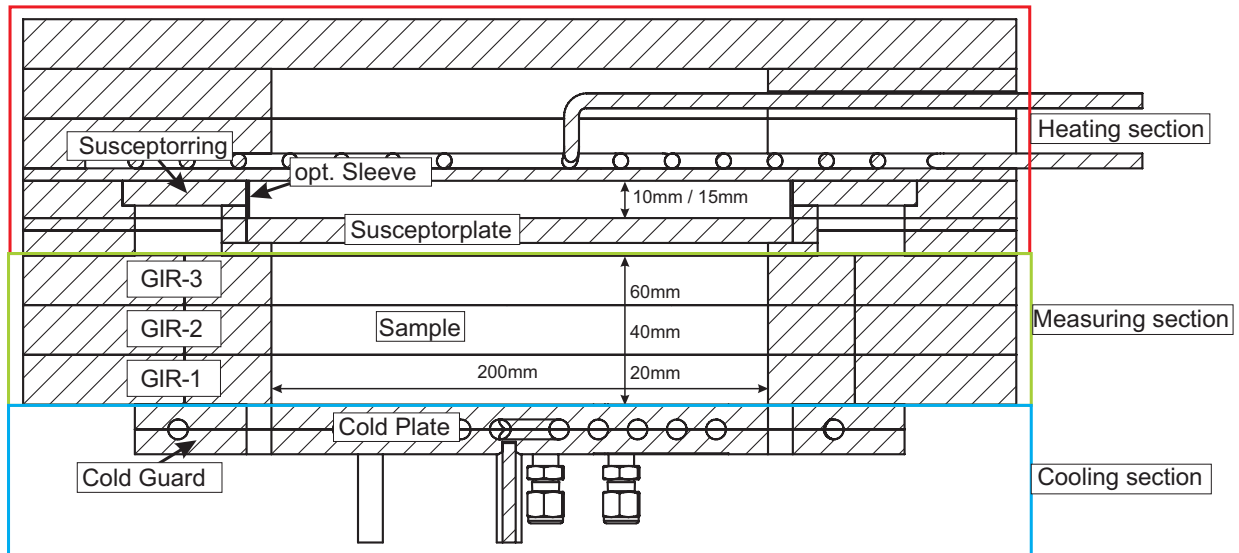


**Fig. 1. Cross-sectional view of HitCon test setup**

means the heat loss or heat gains in radial direction have to be suppressed or, practically speaking, to be minimised. The goal of high measurement accuracy requires further that the temperature gradient has to be large compared to inaccuracies in temperature and dimensional measurements. When the specimen conductivity is low and the heat flux is correspondingly low, only a relatively small thickness is required to generate a large, accurately measurable temperature gradient. With this low specimen heat flux, lateral losses are of concern, thus “flat” plate-type specimen itself tends to minimise these spurious radial flows since the relative size of the lateral surfaces to the cross section becomes small. Another independent parameter of fundamental importance is the magnitude of specimen conductivity relative to the surroundings. This becomes a problem as the temperature of the measurement system rises. In this case the test specimen has to be surrounded by edge insulation to limit radiative and convective losses at the specimen edges.

## 2.1 Measurement Approach Adapted for Hitcon

The test setup developed here is a modified guarded hot plate measurement setup [1] of which a cross-sectional view can be seen in Fig.1. The top side of the sample is heated in the heating section to temperatures up to 1450°C whereas the bottom side is held at temperatures around 40°C by the cooling section. Thus a heat flux through the measuring section is induced, which is measured calorimetrically in the cooling section. The whole test setup is mounted in a vacuum chamber to allow for tests at different ambient pressures. The test setup can be subdivided in three sections, which are briefly described below. A more detailed description is given in [2].

### 1.) The cooling section:

It consists of the Cold Plate (CP) and the Cold Guard (CG) separated by a layer of Pyrogel insulation and equipped with sensors to measure temperatures and heat fluxes. The inlet and outlet temperature of the coolant is measured together with the flow rate to determine the heat flux absorbed by the coolant. This heat flux consists of the heat flux from the test sample, but also of radial heat fluxes from the cold guard and heat fluxes to the bottom side of the cold plate. To minimize the heat flux from the cold guard, the flow rate to the cold guard can be adjusted independently from the cold plate, so that temperatures measured at the edge of CG and CP are very close. Additionally, there are heat flux sensors on top and bottom of the cold plate, which are used to determine the heat flux to the bottom of the cold plate. These heat flux sensors also measure the cold side temperature of the sample.

### 2.) The measuring section:

It consists of the circular test sample surrounded by instrumented guard insulation rings (GIR). Three rings GIR -1 to 3 are used, each with a height of 20mm and equipped with different thermocouples. These thermocouples are installed with a spacing of 120° on different heights and on two radii. Together with the thermal conductivity of the insulation material, this setup allows for correction of the parasitic heat fluxes into or out of the sample.

### 3.) The heating section:

With the heating section, the sample is heated by radiation from the Susceptorplate (SP) and the GIRs are irradiated by the Susceptorring (SR). The SP and SR are inductively heated by a coil on top of the heating section. This setup allows for higher temperatures in the guardrings compared to the sample. With an optional sleeve this temperature difference can be further tuned.

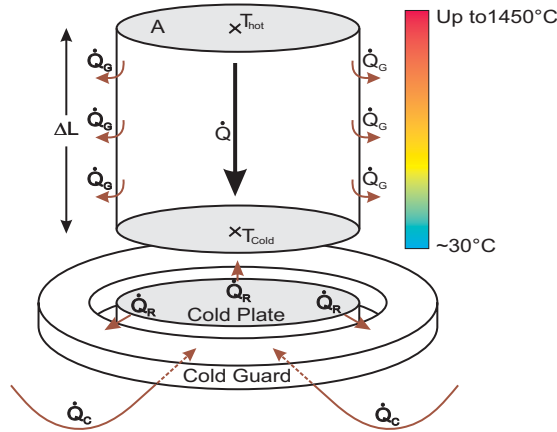


Fig. 2. Schematic heat fluxes in test setup

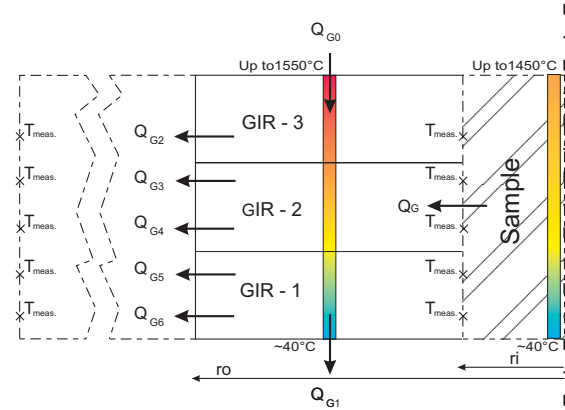


Fig. 3. Control volume for determination of QG

## 2.2 Determination of True Heat Flux through Sample

The calorimetrically measured heat flux in the cold plate is not the true heat flux through the sample, but is falsified by heat exchanges between sample and insulation rings and parasitic heat fluxes to the bottom and the lateral surface of the cold plate. To determine a corrected heat flux a correction algorithm was developed. The heat exchange between sample and insulation rings is determined via measurement of the temperature distribution in the insulation rings. The temperature measurements are done for 3 sections, one section every 120° and with 4 TCs in each section for GIR 1 and GIR 2 and 2 TCs in each section for GIR 3. One of these sections is shown in Fig.3 With known temperature distribution and the thermal conductivity of the insulation rings, Fourier's law [3] gives the heat exchange between sample and insulation rings as

$$\dot{Q}_{GX} = \lambda_{Insulation} \cdot \frac{A_{CV}}{\Delta H} \cdot \Delta T \quad \text{for } X = 0,1 \quad (2)$$

$$\dot{Q}_{GX} = \lambda_{Insulation} \cdot 2 \cdot \pi \cdot H_X \cdot \frac{\bar{T}_{ri} - \bar{T}_{ro}}{\ln(r_o/r_i)} \quad \text{for } X < 1 \quad (3)$$

Summation of the calculated heat fluxes over the control volume results in the heat flux between sample and insulation ring. This method depends on accurate measurement of the temperature field and on a precise knowledge of thermal conductivity of the guard insulation. In view of considerable tolerances in the guard insulation supplier data for temperatures below some 600°C such precision was not fully available for the demonstration test campaign (see Fig.7). Fig.2 illustrates the parasitic heat fluxes  $\dot{Q}_C$  and  $\dot{Q}_R$  to the cold plate. The heat flux  $\dot{Q}_C$  is determined with heat flux measurements  $\dot{q}_{below}$  for measurements to the bottom and  $\dot{q}_{above}$  with measurements to the top of the CP. The ratio of these measurements like

$$\frac{\dot{q}_{below}}{\dot{q}_{above}} = R_{QC} \quad (4)$$

gives the parameter  $R_{QC}$ , which is then used later in the determination of the corrected heat flux (6). The realised test set-up showed that this parasitic flux is generally small except for the nanoporous test specimen. The radial parasitic heat flux is minimised by controlling the water flow rate in the cold guard such that temperature differences across the gap between the cold plate edge and cold guard edge are minimum. Such minimal differences could be achieved in all cases [2]. Nonetheless, the heat flux is determined with temperature measurements on the edge of the cold guard and cold plate. Again, Fourier's Law gives the lateral heat flux as

$$\dot{Q}_R = \lambda_{Pyrogel} \cdot 2 \cdot \pi \cdot l \cdot \frac{\bar{T}_{CP} - \bar{T}_{CG}}{\ln(r_{CG}/r_{CP})} \quad (5)$$

With the so determined parasitic heat fluxes, the corrected heat flux through the sample can be determined as

$$\dot{Q}_{Corrected} = \frac{\dot{Q}_{Calorimetric} - \dot{Q}_R}{1 + R_{QC}} - \dot{Q}_G \quad (6)$$

This corrected heat flux is then used for the determination of the thermal conductivity. From simulations it is expected, that the uncorrected thermal conductivity, determined only with  $\dot{Q}_{Calorimetric}$ , provides a lower boundary for the true thermal conductivity, whereas the corrected thermal conductivity provides an upper boundary.

### 3 ASSESSMENT OF MEASUREMENT RESULTS

#### 3.1 Measurement Uncertainties

While the test is running in steady state, all measured data is recorded constantly. The arithmetic mean of the recorded data is then used to continue with the calculation of the thermal conductivity.

The error is calculated according to [4]. First the empirical standard deviation is calculated as

$$s = \sqrt{\frac{1}{N-1} \cdot \sum_{i=1}^N (Y_i - \bar{Y})^2} \quad (7)$$

With  $N$  the quantity of measurements,  $Y$  the single value of measured data and  $\bar{Y}$  the arithmetic mean of measured data. Because the mean value is used later in the determination of the thermal conductivity, the standard error of the arithmetic mean needs to be determined. This can be done using the Student's t-distribution. The standard error  $\Delta\bar{Y}_{emp}$  of the arithmetic mean is

$$\Delta\bar{Y}_{emp} = \frac{s}{\sqrt{N}} \cdot t \quad (8)$$

where  $t$  considers the uncertainty of  $s$ . Its value depends on the level of confidence and the number of measured data. The level of confidence is set to 99%. Finally the confidence interval of the arithmetic mean for the measured mean values is given as

$$\bar{Y} \pm \Delta\bar{Y}_{emp} \quad (9)$$

The error of the measured values leads to an error in further calculations. To determine this uncertainty standard error propagation is used as in

$$\Delta\bar{Z} = \sqrt{\left(\sum_{j=1}^k \left(\frac{\partial f}{\partial Y_{emp,j}} \cdot \Delta Y_{emp,j}\right)^2\right)} \quad (10)$$

with  $\Delta\bar{Z}$  the standard error of the calculated value and  $\partial f / \partial Y_{emp,j}$  the partial derivative. The uncertainties considered for this error propagation are tabulated in Table 2. Additional uncertainties stem from the height and diameter measurements of the sample. These uncertainties are for the current measurements estimated with a rather high value, because the samples available were inclined. Especially interesting is the influence of the sample height uncertainty, which is shown exemplarily for Saffil in Table.1. It can be seen, that the uncertainty in thermal conductivity and mean temperature stems almost exclusively from the uncertainty considered for the geometric measurements. With non-inclined samples, this uncertainty should be considerably smaller. With the help of the error propagation introduced in (10), the standard error of the overall results can be estimated.

**Table 1. Uncertainties of measurements depending on geometrical uncertainties**

mean Temperature	uncertainty in mean temperature		uncertainty in corrected thermal conductivity	
	only emp. standard deviation	with uncertainty in diameter and height	only emp. standard deviation	with uncertainty in diameter and height
572,9 °C	0,011 °C	81,3 °C	0,0002 W/(m*K)	0,008 W/(m*K)
868,6 °C	0,015 °C	107,7 °C	0,0004 W/(m*K)	0,012 W/(m*K)
995,2 °C	0,018 °C	118,1 °C	0,0011 W/(m*K)	0,013 W/(m*K)

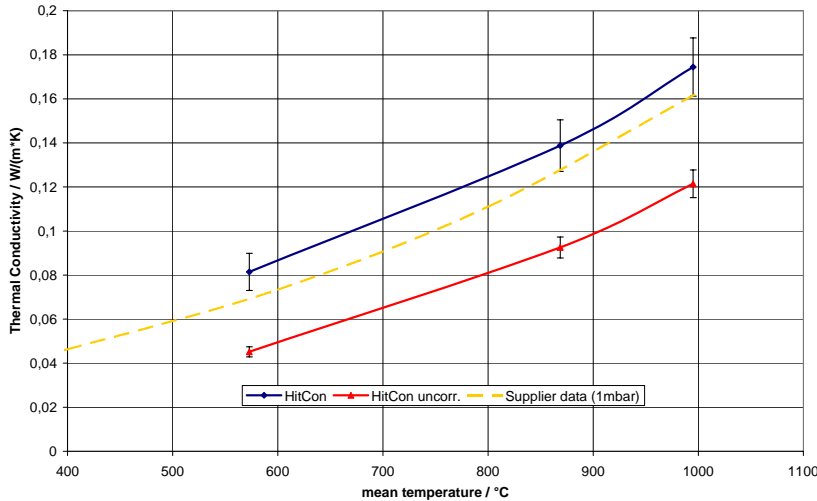


**Fig. 4. Measurement results for Saffil**

### 3.2 Measurement results for Saffil

Saffil is an alumina fibre insulation and serves as reference measurement. FIG.4 compares the HitCon measurements on aluminium fibre insulation with insulation data received from the supplier. The supplier data were available as analytical fits to various thermal conductivity measurements for different temperatures, pressures and densities. All measurements in the HitCon facility for the Saffil insulation were performed at pressure levels of 0.4 mbar to 1.9 mbar. What is shown is the uncorrected, apparent thermal conductivity measured (“HitCon uncorr.”), where the correction algorithm was not used. All 3 measured apparent thermal conductivities are below the supplier data. The temperature trend of apparent conductivities is similar to the supplier data. When the off-line correction is applied (“HitCon”), the apparent thermal conductivities values are shifted to higher values, which are now above the supplier data at 1 mbar reduced pressure. The difference is approximately 13% for the lowest measured temperature with decreasing trend to higher temperatures. As expected, the uncorrected thermal conductivity provides a lower, and the corrected thermal conductivity provides an upper boundary for the “true” thermal conductivity. In summary, the HitCon measurements on Saffil after correction fit favourably well with supplier derived data.

### 3.3 Measurement results for IMI

IMI (Internal Multiscreen Insulation) is an anisotropic insulation and is among the most advanced insulation concepts. The justification for measurements on such an insulation type was to demonstrate that the HitCon apparatus is applicable to this type of insulation, which was one of the major drivers for the development of the HitCon facility. IMI consists of highly reflective gold coated ceramic screens separated by low density fibre spacers, providing the anisotropic thermal conductivity. The transversal conductivity (perpendicular to the screens) will be smaller than the in-plane conductivity. The thermal conductivity of such an insulation can no longer be determined by the hot wire test method contrary to homogeneous insulations. The measurements were conducted perpendicular to the gold screens, for different temperatures at 1 mbar pressure and one temperature at 900 mbar pressure. The results can be seen in Fig.5. Again, the uncorrected results at 1 mbar pressure are below the supplier data and are shifted by the correction to higher values, only slightly above the supplier data. For the measurement at 900 mbar, the uncorrected values are again, but this time only slightly, below the supplier data. The correction shifts the result again to a higher value. Again, the assumption that the uncorrected measurements provide a lower and the corrected measurements an upper boundary is confirmed. In summary, the HitCon measurements on IMI after correction fit well with data derived from a supplier validated model for low pressures, but the measurement at 900 mbar needs improvement.

**Table 2. Uncertainties for error propagation**

Parameter	Uncertainty considered
All temperatures	standard deviation
Pressure	standard deviation
Heat fluxes	standard deviation
Sample height	2mm
Sample diameter	1mm

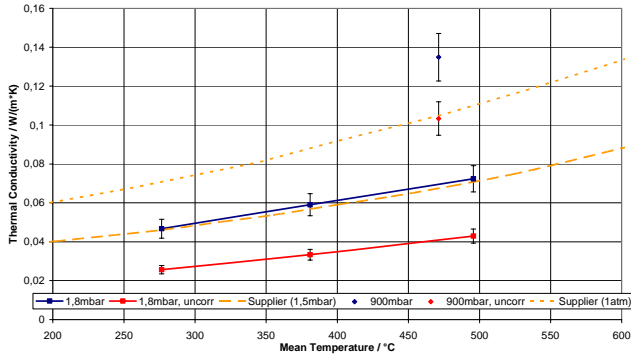


Fig. 5. Temperature dependent results for IMI

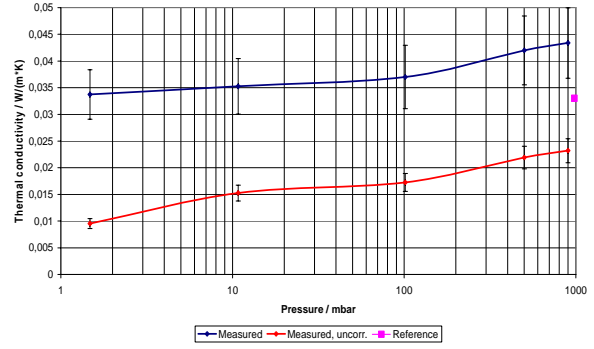


Fig. 6. Pressure dependent results for Pyrogel

### 3.4 Measurement results for Pyrogel

Pyrogel is a flexible nanoporous insulation. It is another kind of advanced insulation material under development since a few years. Due to the small pore size the residual conductivity of enclosed air is below the conductivity of still air already at normal pressure levels (i.e.  $\sim 1013$  mbar). Fig.6 illustrates the pressure dependency of the measured thermal conductivities. The pressure dependency of thermal conductivity is physically correctly reflected. The available Pyrogel is a two component blend of fibres and pure aerogel, i.e. comprises two different pore patterns. This is clearly observed in the HitCon measurements, which present two levels of thermal conductivity reductions with decreasing pressure. The first decrease is due to “evacuation” of the nanopores in the aerogel and the second one is due to “evacuation” of the micropores in the fibre lattice. For the apparent thermal conductivity  $\sim 14$  mW/(m $\cdot$ K) reduction were measured in the HitCon facility at further reduced pressure of approximately 1 mbar. This reduction shrinks to only  $\sim 10$  mW/(m $\cdot$ K) after correction. A second reduction of thermal conductivity at 1 mbar is in agreement with the trend observed in other facilities and with theoretical explanations (mix of two distinct pore sizes). In summary, basically the pressure dependence of the Pyrogel insulation as measured in the HitCon apparatus favourably matches the trend of other measurement results, but the apparent thermal conductivities are too low and the corrected thermal conductivities may be slightly too high.

## 4 SENSITIVITY EXAMINATION

From the above results it is obvious, that, although the principle of the measurement with the offline-correction is feasible and already produces reasonable results, there is also potential for improvement. In order to identify the most important points for improvement, a sensitivity analysis was performed. As the parasitic heat flux through the GIR is the most important correction, the sensitivity with regard to thermal conductivity of the GIRs was determined first. The thermal conductivity of the GIRs in air at standard ambient pressure has been provided by the insulation supplier, the pressure dependency was developed during calibration measurements. This data was then fitted to an equation the form of

$$\lambda(p,T) = \lambda(1013\text{mbar},T) - \lambda_{air}(T) + \lambda_{air}(T) \frac{1}{1 + C \cdot (273 + T) / p} \quad (11)$$

However, for lower temperatures below  $600^\circ\text{C}$  the data is uncertain, due to differing data sets received from the supplier. Both data sets at atmospheric pressure are shown in Fig.7, the first one as the lower fit, the other is shown as the upper fit.

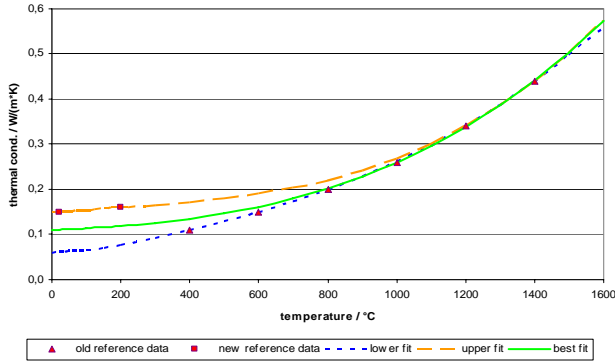


**Fig. 7. Guard insulation thermal conductivity**

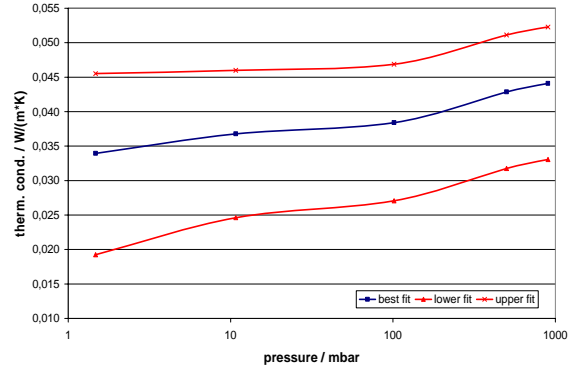


**Fig. 8. Sensitivity on GIR thermal conductivity**

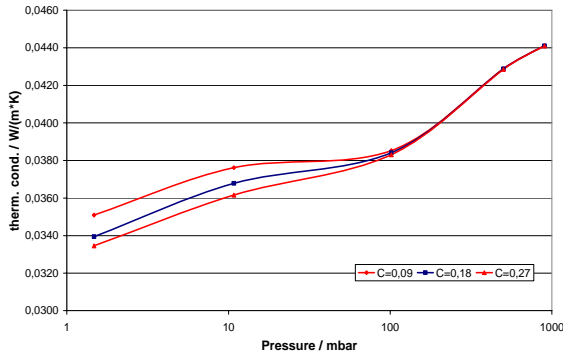


**Fig. 9. Sensitivity on GIR pressure dependency**

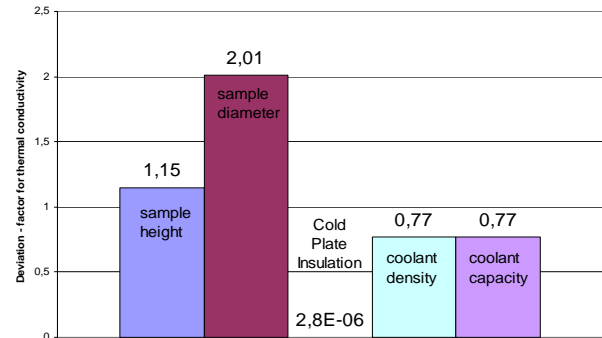


**Fig. 10. Deviation factors**

The differences may be caused by applying different thermal conductivity measurement methods. However, it is not obvious which one is better and in order to minimize potential errors a best fit between original and recent supplier data was used for the thermal conductivity of the GIRs. The uncertainty which results for the measured thermal conductivity in the sample was determined during the sensitivity analysis, where the measurements were evaluated with the “best” fit of DLR to original/recent supplier data and with an “upper” fit (overweighting recent supplier data) and a “lower” fit (emphasising original supplier data). These three fits are illustrated exemplarily for Pyrogel in Fig.8. The “lower” fit results in thermal conductivities up to 40% lower than with the best fit. The “upper” fit results in thermal conductivities up to 30% higher than with the best fit. Pyrogel is the best insulation tested and is therefore also the one with the highest sensitivity with regard to GIR thermal conductivity. In our understanding this uncertainty is a worst case result, but further testing and independent measurement of GIR thermal conductivity is necessary. To get the sensitivity on pressure dependency, the factor  $C$  in (11) was varied. The results are shown in Fig.9. As can be seen, there is a difference below approximately 100 mbar. But these differences are with about 3% rather small.

Next the sensitivities in regard to sample height and diameter, thermal conductivity of CP insulation and coolant density and capacity were determined. Therefore the measurements have been evaluated with differences in these parameters of 0.1 %, 1 % and 10 %. To get a simple mean to assess the sensitivity a deviation factor has been defined as the ratio of the deviation in thermal conductivity of the sample in percent and the deviation in percent of the studied parameter.

$$D = \frac{\Delta\lambda_{Sample} [\%]}{\Delta Parameter [\%]} \quad (12)$$

The highest of these deviation factors are summarized in Fig.10. For the thermal conductivity the sample diameter has the biggest influence on the results, where a sample diameter error of 10% results in more than 20% error in thermal conductivity. Together with the sample height, this value must be measured on the actual sample, which might be difficult because of the fibrous and flexible nature of the insulations and possible changes during measurements at high temperatures. The coolant density and capacity are also important, but as the coolant is water, these values are well known with good accuracy. The least important point is the thermal conductivity of the CP insulation. In our opinion the reason for this is, that the parasitic heat flux to the CP is rather small. This examination was also done for the determination of the mean temperature. Here the only parameter with an influence was the sample height, where deviation

factors of up to  $D=0.6$  were found. That sample height is here the only examined factor that has an influence on the mean temperature, agrees well with the findings from the error propagation, where the uncertainty in mean temperature was almost exclusively caused by the uncertainty in height measurements.

## 5 CONCLUSIONS

The thermal conductivity measurements performed in the HitCon facility had not the goal to determine insulation conductivities precisely. The prime objective was to check the proper construction of the facility, the adequacy of the proposed approach and the exploration of the operational regime for different types of insulations. Any comparison performed within this program has to be considered as a check whether HitCon measurements yield reasonable results. Indeed it was found that thermal conductivities could be measured in the HitCon apparatus with significantly higher accuracy than with the approach followed during a previous project [5]. Measurements performed in the operation demonstration campaign revealed test results which favourably compare to available data for three different insulation types. The expectation that the measured “apparent” conductivities and the “corrected” conductivities provide a lower and an upper envelope for the “true” thermal conductivities was confirmed. It should be pointed out that the “corrected” conductivities depend strongly on the thermal conductivity of the guard insulation itself. Unfortunately, the latter input is at present only known with considerable tolerance for temperatures below  $\sim 600^{\circ}\text{C}$ . The first step to further improve the measurements is therefore to gather more accurate thermal conductivity data for the guard insulation at temperatures below  $600^{\circ}\text{C}$  and different pressures. The error analysis and sensitivity examination also clearly showed the importance of accurate measurement of the sample height and diameter.

## 6 REFERENCES

- [1] ISO 8302:1991, Thermal insulation - Determination of steady-state thermal resistance and related properties - Guarded hot plate apparatus, 1991
- [2] M. Selzer, K. Keller, T. Reimer, „HitCon - Final Report“, unpublished
- [3] F. P. Incropera, D. P. DeWitt, “Fundamentals of Heat and Mass Transfer”, *John Wiley & Sons, Inc.*, 1996
- [4] J. Hoffmann, F. Adunka, „Taschenbuch der Messtechnik“, *Hanser Verlag*, 2007
- [5] IHST-DLR-RP-0003, issue 1, 17.12.2004